Atienza, F.; Climent, A.; Guillem Sánchez, MS.; Berenfeld, O. (2015). Frontiers in Non-invasive Cardiac Mapping: Rotors in Atrial Fibrillation-Body Surface Frequency-Phase Mapping. Cardiac Electrophysiology Clinics. 7(1):59-69. doi:10.1016/j.ccep.2014.11.002

Published in final edited form as:
Card Electrophysiol Clin. 2015 March 1; 7(1): 59–69. doi:10.1016/j.ccep.2014.11.002.

Frontiers in Non-invasive Cardiac Mapping: Rotors in Atrial Fibrillation-Body Surface Frequency-Phase Mapping

Felipe Atienza, MD[&], **Andreu M Climent, PhD**[&], **María S Guillem, PhD**[§], and **Omer Berenfeld, PhD, FHRS**[#]

[&]Hospital General Universitario Gregorio Marañón, Madrid, Spain

[§] Bio-ITACA, Universitat Politécnica de Valencia, Valencia, Spain

[#]Center for Arrhythmia Research, University of Michigan, Ann Arbor, Michigan

Abstract

Experimental and clinical data demonstrate that atrial fibrillation (AF) maintenance in animals and groups of patients depends on localized reentrant sources localized primarily to the pulmonary veins (PVs) and the left atrium(LA) posterior wall in paroxysmal AF but elsewhere, including the right atrium (RA), in persistent AF. Moreover, AF can be eliminated by directly ablating AF-driving sources or "rotors," that exhibit high-frequency, periodic activity. The RADAR-AF randomized trial demonstrated that an ablation procedure based on a more target-specific strategy aimed at eliminating high frequency sites responsible for AF maintenance is as efficacious as and safer than empirically isolating all the PVs.

In contrast to the standard ECG, global atrial noninvasive frequency analysis allows non-invasive identification of high-frequency sources before the arrival at the electrophysiology laboratory for ablation. Body surface potential map (BSPM) replicates the endocardial distribution of DFs with localization of the highest DF (HDF) and can identify small areas containing the high-frequency sources. Overall, BSPM had a sensitivity of 75% and specificity of 100% for capturing intracardiac EGMs as having LARA DF gradient. However, raw BSPM data analysis of AF patterns of activity showed incomplete and instable reentrant patterns of activation. Thus, we developed an analysis approach whereby a narrow band-pass filtering allowed selecting the electrical activity projected on the torso at the HDF, which stabilized the projection of rotors that potentially drive AF on the surface. Consequently, driving reentrant patterns ("rotors") with spatiotemporal stability during >70% of the AF time could be observed noninvasibly after HDF-filtering. Moreover, computer simulations found that the combination of BSPM phase mapping with DF analysis enabled the discrimination of true rotational patterns even during the most complex AF. Altogether, these studies show that the combination of DF analysis with phase maps

Corresponding Author: Omer Berenfeld, PhD, FHRS Center for Arrhythmia Research 2800 Plymouth Rd. Ann Arbor, MI 48109 Phone: (734) 998-7560 oberen@umich.edu.

Drs. Atienza, Climent, and Guillem have nothing to disclose.

of HDF-filtered surface ECG recordings allows noninvasive localization of atrial reentries during AF and further a physiologically-based rationale for personalized diagnosis and treatment of patients with AF.

Keywords

Atrial fibrillation; Body surface mapping; Rotors; Dominant frequency Fourier transform; Phase mapping

Introduction

Atrial fibrillation (AF) is the most common arrhythmia seen in clinical practice and is associated with increased risk of stroke, heart failure and death.[1] Although antiarrhythmic drugs have limited efficacy, the demonstration of AF triggers in the atrial sleeves of the pulmonary veins (PVs) has led to a significant improvement in therapy.[2, 3]

Several ablative strategies have been developed with the objective of creating circumferential lesions around the PV ostia.[4] Empiric circumferential pulmonary vein isolation (CPVI) is effective in ~70-80% of patients with paroxysmal AF and has become therapy of choice for drug-refractory AF in these patients.[5] However, results still remain suboptimal due to the presence of non-PV sources maintaining AF.[4, 6, 7] Moreover, the success rate of CPVI in the more prevalent persistent and long-lasting AF populations is significantly lower and extensive substrate based ablation strategies have been used with conflicting results.[8, 9]

Experimental and clinical data from our laboratory support the hypothesis that both acute and persistent AF in the sheep and some groups of human patients is not a random phenomenon. Studies analyzing the spatiotemporal organization of waves and dominant frequency (DF) in the isolated sheep heart demonstrate that AF maintenance in this model depends on localized reentrant sources in the left atrium (LA) and fibrillatory conduction in its periphery.[10-15]As a natural consequence of these studies, we translated the analysis on the organization of DF to human AF and found that AF reentrant sources are localized primarily to the PVs and LA posterior wall in the case of paroxysmal AF but elsewhere in the case of persistent AF.[16-20] Several of these observational studies showed that AF could be eliminated by directly ablating AF-driving sources or “rotors,” that exhibit high-frequency, periodic activity, based on either electrogram visual analysis, dominant frequency analysis or panoramic endocardial mapping.[2, 17-19, 21-25] Recently the first randomized clinical trial, RADAR-AF, demonstrated that in paroxysmal AF patients, selective ablation of sites responsible for AF maintenance is as effective as CPVI, and decreased ablation risks.[26] These results demonstrate that a an ablation procedure based on a more target-specific strategy aimed at eliminating high frequency sites responsible for AF maintenance is as efficacious and safer than empirically isolating all the PVs.

Therefore, it would be arguably desirable to noninvasibly both identify the location of the sources responsible for AF maintenance before the procedure in order to design the ideal ablation strategy for each individual AF patient as well as to be able to perform a panoramic

real-time localization of sources during the procedure.[27, 28] Although the highest frequency sources in paroxysmal AF are most commonly located in the junction of the left atrium with the PVs, they have also been identified elsewhere in the atria and may shift in time. Recent studies by our group have shown that panoramic, global, atrial noninvasive frequency analysis is feasible in AF patients and may allow the identification of high-frequency sources before the arrival at the electrophysiology laboratory for ablation. Body surface map (BSPM) replicates the endocardial distribution of DFs and can identify small areas containing the high-frequency sources that result in fibrillatory conduction to the reminder of the atria, and may decrease the time required for the search and elimination of the highest DF (HDF) site.[29] Moreover, we recently have shown that phase maps of surface potentials during AF after HDF-filtering allow observing driving reentrant patterns ("rotors")with spatiotemporal stability during >70% of the AF time.[30]Thus, as will be shown in the following sections, the ability of BSPM to detect site(s) driving AF may enable a noninvasive personalized diagnosis and treatment of patients with AF.

The non-invasive mapping system

In our studies, AF patients wore a custom-made, adjustable vest with 64 electrodes covering the entire torso surface (Figure 1) during the ablation procedure.[17, 29, 30] The vest included recording electrodes on the anterior (N=28), posterior (N=34) and lateral sides (N=2) of the torso. In addition, three limb leads were recorded and used to generate the Wilson Terminal. The BSPM vest was placed prior to the catheterization and fastened anteriorly, allowing access to the patient chest in case external electrical cardioversion was needed during the course of the study. Surface unipolar electrocardiographic recordings were obtained by using a commercial system for bio-potential measurements (Active Two, Biosemi, The Netherlands) at a sampling frequency of 2048 Hz and stored on hard disk for off-line analyses.[31] Ventricular activity was removed from the unipolar recordings prior to analysis either numerically, or by application of adenosine.[29]

Spectral analysis of body surface potential mapping

Previous studies have highlighted the major role of maximal DF (DFmax) sources in the maintenance of AF in animals and humans.[14, 17, 32] Arguably, prior knowledge of which atrium harbors the DFmax source that maintains the arrhythmia may allow better planning of the ablation procedure, and may accelerate the intracardiac localization of the highest DF point and reduce ablation time. Thus we explored the ability of the body surface DFs to capture the intracardiac DFmax.

Surface leads and simultaneously recorded intracardiac signals presented closely related spectral components. In Figure 2 we present spectral analyses of data from a representative patient in whom the presence of distinct atrial site with high-frequency activity in the posterior LA could be determined noninvasively. In Figure 2A, three representative EGMs illustrate the range of activation rates across the atria, with DFs ranging from 5.75 Hz in the RA to 7 Hz in the LA near the left superior pulmonary vein (LSPV). Simultaneously recorded surface leads also showed different DFs at nearly the same frequency range found in the EGM recordings, as shown in Figure 2B by three representative leads corresponding to the surface left (SL), surface posterior (SP) and surface right (SR) regions. Surface DFs

mostly correlated with the activation rate of nearest atrial tissue: the highest endocardial DF point was observed at the nearest point on the torso surface (central posterior) and the lowest activation rate of the RA was found at the nearest portion of the surface ECG (right inferior). Intracardiac CARTO DF maps obtained prior to adenosine infusion and surface DF distributions obtained during adenosine infusion showed good correspondence (Figure 2C and 2D), but a direct comparison of frequencies from CARTO and surface maps was unattainable due to its sequential nature and because adenosine accelerates AF activation in humans.[18].

In panels A and B of Figure 3, we display difference maps obtained by subtracting DF values on the surface map from the intracardiac DFmax in patients from Figures 2 and another patient in which the DFmax resides in the RA. In each case, the white arrow points to the red color DFmax domain on the surface, which corresponds to the region with zero difference with the intracardiac DFmax. These examples demonstrate that the surface DFmax can accurately detect the value of the intracardiac DFmax value, regardless of whether the latter is localized to the LA or the RA. To further analyze the correspondence between intracardiac and surface AF frequencies in the RA and LA we grouped the intracardiac DFmax values measured in the LA and RA and correlated them with the DFs of EGMs from matching portions on the body surface. These matching portions were defined as those in which the difference between the intracardiac DFmax in each atrium and the surface DFmax was ≤0.5 Hz. Panels C and D of Figure 3 show that when the entire patient population under study was included, there was a good correspondence between maximum DFs found in each atrial chamber and right and left matching portions of the body surface, respectively. The correlation between right surface leads and right intracardiac EGMs was 0.96, whereas correlation for left leads with left intracardiac EGMs was 0.92 (Figure 3E and 3F). The attempted correlation of surface leads with EGMs of the opposed atrial chamber yielded much lower correlation values (RA body surface leads vs intracardiac LA EGMs, 0.26; one tail t-test after Fisher r-to-z transform: $p<0.0001$ vs. $r=0.96$; left body surface leads vs intracardiac RA EGMs, 0.46; $p=0.0052$ vs. $r=0.92$).

Such a strong, side-specific correspondence of frequencies enabled reliable determination of atrial frequency gradients non-invasively.[29]The DF gradients on the 64 electrodes of the BSPM showed a good correlation with the DF gradients obtained by the simultaneous intracardiac EGMs (correlation coefficient = 0.93). On the other hand, surface frequency gradients estimated by the standard precordial ECG leads yielded a poor correspondence with gradients estimated from the intracardiac EGMs, with a correlation coefficient equal to 0.41 when considering all 6 standard leads, or equal to 0.51 when considering only V1 and V6 ($p=0.0051$ when compared with the correlation of the full BSPM DF gradients).[27, 29]

To predict the ability of the BSPM to detect intracardiac LA-to-RA DF gradients, we classified patients with a LA-RA gradient in DF (maximal right and left values differ by more than 0.5 Hz) versus without LA-RA gradient, otherwise. Overall, the sensitivity of the BSPM to capture intracardiac EGMs as having LA-RA gradient in DF was 75%, but the specificity of the BSPM in capturing those gradients was 100%. The sensitivity and specificity of the standard ECG leads V1 and V6 in detecting a LA-to-RA DF gradient were 67% and 50% respectively. In other words, while the BSPM was able to identify most, but

not all, intracardiac DF gradients, each DF gradient identified by the BSPM was a true gradient as determined by the intracardiac recordings. Standard ECG leads, however, allowed the detection of a lower proportion of patients with LA-to-RA DF gradients as compared to all BSPM leads and also mistakenly identified LA-RA DF gradients that were not confirmed in the EGM recordings.

Surface mapping of atrial patterns of activity during AF

Surface phase maps of the unipolar voltage time-series recorded during AF show unstable patterns, as can be appreciated by the transient singularity points (SPs) seen in the maps from a sample patient presented in the left panel of Figure 4A.[30] Long-lasting SPs were rarely observed during AF without band-pass filtering and those observed tended to drift erratically large distances in short time. However, after bandpass filtering of the potential signal around the HDF (6.8 Hz), surface phase maps showed more stable SPs for the same AF episode (Figure 4A, right panel). In Panel B the arrows connecting sequential activations in ECGs recorded around the SP in Figure 4A show a clear reentrant pattern which following HDF-filtering transformed into long-lasting rotational patterns with stable SPs. Considering data from all patients, stable SPs were found in unfiltered AF signals during 8.3±5.7% of the time vs. 73.1±16.8% following HDF-filtered signals ($p<0.01$). The average SPs' duration concomitantly increased following the HDF-filtering (160±43 vs. 342±138 ms, $p<0.01$). At an average HDF of 9.2±2.3 (BSPM) or 9.3±2.0 (EGM) Hz, the latter corresponds to an average of 2.9±0.7 continuous rotations per SP observed in our cohort of 14 patients.[30] Many observed SPs drift and appear or disappear on the borders of the surface mapped area, or in the beginning and end of the periods analyzed, thus this average number of rotations represents a lower limit for their life span. Indeed, Figure 4C and Video 1 (available online at http://www.cardiacep.theclinics.com/). show a rotor in the middle of the mapped area at the beginning of the period analyzed that after about 1400 ms disappears at the lower boundary of the area. After a period of fuzzy SP behavior in the posterior torso (see Video 1) for about 330 ms, an SP appears and remains in the mapped area for the rest of the analyzed period. This case shows that the actual life span of rotors could be longer than the conservative average life-span we calculate. Further evidence of atrial rotor drifting is provided by the simultaneous EGM recorded at the highest DF site (Figure 4E), which is unstable in intervals 1-4 and monomorphic at interval 4-5, which is consistent with the observed drifting on the torso surface.

Simulations to understand HDF band-pass filtering of AF patterns

The finding that the dynamics of the body surface SPs dramatically depends on the HDF-filtering raises questions regarding the phase maps interpretation. Unfortunately, the ability to collect simultaneously electrical data in the atria and inside the torso volume and surface to make inferences between atrial activity and its manifestation on the body surface is limited, leading us to rely on computer simulations for guidance.

In Figure 5 a simulation with a LA–RA atrial model and the multi-spheres torso model is depicted. In this model there is a single functional rotor in the LA hemisphere turning at 7.2 Hz while the RA hemisphere is passively activated at lower a frequency (3.9 Hz). Figure 2A shows the phase maps of three concentric layers between the epicardium (left) and the torso

surface (right) at various times. The phase maps become smoother toward the torso surface, reflecting the low-pass filter effect of the passive torso volume on the extracellular potentials. In the epicardial layer there is one stable SP at the location of the functional rotor (LA) that appears at similar positions in the outer layers, and another SP at the less stable wavebreak location at the interface between the faster LA and the slower RA. Azimuth and elevation of SPs detected on the surface are not preserved across layers, so the filament arising from the LA rotor exhibits a deflection in its trajectory to the torso. The deflection angle of the filaments before HDF-filtering is not stationary over time and, instead, the filament trajectory describes a cone. However, Figure 5B shows that HDF-filtering significantly reduces the filaments' deflection and stabilizes them to follow a straight path from the epicardium to the surface. The simulations suggested that SPs arising at the interface between LA and RA as a consequence of abrupt changes in propagation direction that reached the outermost layer disappear after HDF-filtering since their activation frequencies did not match with the HDF.[30] In addition, we notice that a mirror filament appears with opposite direction and chirality as compared to the true rotor originating at the SP on the LA epicardium. Indeed, following the attenuation of RA activation frequencies, potentials on the RA hemisphere are caused by the rotating electrical activity on the LA and observed from a contralateral point of view.

The torso as a low-pass filter for rotor activity

We further explore the behavior of filaments under more complex wave patternsresulting from a 50% LA area and 50% fibrotic area model.[30] In this case epicardial activity consists of a LA rotor with a stable SP and a highlydisorganized activity with several unstable SPs in the fibrotic area. Most of the filaments originate at SPs involving a small piece of fibrotic tissue and not at the driving rotor. In that case the torso volume conductor stabilizes filaments and eliminates all but a single filaments' pair reaching the surface. Our simulations clearly show that filaments are continuous and do not vanish inside the passive volume conductor, rather a filament does not reach the surface once it is joining its counter-rotating neighbor. Overall, that mutual cancelation of filament pairs reduces the average number of SPs at increasing distances from the epicardium.

But as shown in Figure 5, only one of the SPs on the body surface is a "true" SP corresponding to a driving rotor, and others are termed "mirror" SPsas they appear following the extinction of an SP at the LA-RA interface as shown in Figure 5, or extinction of SPs in fibrotic area, with an extension of the stable LA rotor filament to the contralateral aspect of the torso.[30] Indeed, the discrimination between true and mirror SPs can be performed based on the spectral properties of surface recordings. Although on the phase map these SPs seem undistinguishable; the spectral power at the HDF, the rotor frequency band,should be maximal only at "true" SPs.[30]

Regions of body surface rotational activity in human AF (filaments)

True SPs detected, defined as those with at least 60% of their spectral content at the HDF band, tended to concentrate at certain torso areas. In Figure 6A, the trajectory of a surface SP that drifted during 2 seconds on the posterior torso of a patient following LAHDF filtering (band-pass filtering at the HDF found in simultaneous left intracardiac EGMs

recordings) is depicted (see Video 1). In Figure 6B the trajectory of a SP that drifted during 500 ms on the right anterior torso in another patient after RA-HDF filtering is shown (see Video 2, available online at http://www.cardiacep.theclinics.com/). In Figure 6C, the 2-dimensional histogram of "true" SP locations after LA-HDF filtering in patients with an inter-atrial DF gradient>1 Hz (n=10) shows a predominant location of SPs on the posterior torso. The 2-dimensional histogram of "true" SP locations after RAHDF filtering in patients with inter-atrial DF gradient shows a predominant localization on the right anterior torso, Figure 6D. The locations of the maximal numbers of true LA or RA SPs (dark red regions) are shown in Panels C and D to reside well within the areas demarcated by the HDFs originating either at the LA or RA, respectively, based on our previous surface-atrial DF distribution correlation study.[29]

Conclusion and Clinical Implications

Global atrial non-invasive frequency analysis is feasible in AF patients and may allow the identification of high frequency sources prior to the arrival at the electrophysiology laboratory for ablation. Importantly, our results lead to the conclusion that, unlike high-resolution BSPM, the standard precordial ECG leads alone are not a useful tool when attempting to localize the site of DFmax sites responsible for AF maintenance.

Our clinical-computational BSPM study on patterns of activity suggests that the body surface data on wavebreaks during AF is incomplete, but it contains features that can be linked to reentrant drivers of AF. We developed an approach whereby a narrow band-pass filtering allows selecting the electrical activity projected on the torso at the HDF, which stabilizes the projection of rotors that potentially drive AF on the surface. Phase maps of HDF-filtered surface ECG recordings may allow the noninvasive localization of atrial re-entries during AF, enabling further physiologically-based rationale for considering the constraints of the inverse solutions.

Thus, our approach of a full panoramic BSPM procedure may help in planning and performing ablation procedures, decreasing the amount of time required for the search of AF drivers. The approach could arguably be used in patient selection since patients without inter-chamber DF gradient or clear localized drivers have lower ablation success rates.[17] Additionally, *a priori* knowledge of the chamber responsible of the maintenance of the arrhythmia in those patients presenting a DF gradient may help in planning and performing the ablation procedure, decreasing the time required for the search and elimination of drivers and/or the highest DF site.

Supplementary Material

Refer to Web version on PubMed Central for supplementary material.

Acknowledgments

Dr. Berenfeld reports research grants and donations from Medtronic and St. Jude Medical. He is a scientific officer and shareholder for Rhythm Solutions, Inc.

References

1. Wann LS, Curtis AB, January CT, et al. Members AATF. 2011 ACCF/AHA/HRS focused update on the management of patients with atrial fibrillation (updating the 2006 guideline): A report of the american college of cardiology foundation/american heart association task force on practice guidelines. Circulation. 2011; 123:104–123. [PubMed: 21173346]
2. Dobrev D, Nattel S. New antiarrhythmic drugs for treatment of atrial fibrillation. Lancet. 2010; 375:1212–1223. [PubMed: 20334907]
3. Haissaguerre M, Jais P, Shah DC, et al. Spontaneous initiation of atrial fibrillation by ectopic beats originating in the pulmonary veins. N.Engl.J Med. 1998; 339:659–666. [PubMed: 9725923]
4. Calkins H, Kuck KH, Cappato R, et al. 2012 hrs/ehra/ecas expert consensus statement on catheter and surgical ablation of atrial fibrillation: Recommendations for patient selection, procedural techniques, patient management and follow-up, definitions, endpoints, and research trial design. Europace. 2012; 14:528–606. [PubMed: 22389422]
5. Pappone C, Oreto G, Rosanio S, et al. Atrial electroanatomic remodeling after circumferential radiofrequency pulmonary vein ablation - efficacy of an anatomic approach in a large cohort of patients with atrial fibrillation. Circulation. 2001; 104:2539–2544. [PubMed: 11714647]
6. Lin YJ, Tai CT, Kao T, et al. Frequency analysis in different types of paroxysmal atrial fibrillation. J.Am.Coll.Cardiol. 2006; 47:1401–1407. [PubMed: 16580528]
7. Lin WS, Tai CT, Hsieh MH, Tsai CF, Lin YK, Tsao HM, Huang JL, Yu WC, Yang SP, Ding YA, Chang MS, Chen SA. Catheter ablation of paroxysmal atrial fibrillation initiated by non-pulmonary vein ectopy. Circulation. 2003; 107:3176–3183. [PubMed: 12821558]
8. Haissaguerre M, Sanders P, Hocini M, Takahashi Y, Rotter M, Sacher F, Rostock T, Hsu LF, Bordachar P, Reuter S, Roudaut R, Clementy J, Jais P. Catheter ablation of long-lasting persistent atrial fibrillation: Critical structures for termination. Journal of cardiovascular electrophysiology. 2005; 16:1125–1137. [PubMed: 16302892]
9. Weerasooriya R, Khairy P, Litalien J, Macle L, Hocini M, Sacher F, Lellouche N, Knecht S, Wright M, Nault I, Miyazaki S, Scavee C, Clementy J, Haissaguerre M, Jais P. Catheter ablation for atrial fibrillation: Are results maintained at 5 years of follow-up? Journal of the American College of Cardiology. 2011; 57:160–166. [PubMed: 21211687]
10. Berenfeld O, Mandapati R, Dixit S, et al. Spatially distributed dominant excitation frequencies reveal hidden organization in atrial fibrillation in the langendorff-perfused sheep heart. J.Cardiovasc.Electrophysiol. 2000; 11:869–879. [PubMed: 10969749]
11. Berenfeld O, Zaitsev AV, Mironov SF, Pertsov AM, Jalife J. Frequency-dependent breakdown of wave propagation into fibrillatory conduction across the pectinate muscle network in the isolated sheep right atrium. Circ.Res. 2002; 90:1173–1180. [PubMed: 12065320]
12. Kalifa J, Tanaka K, Zaitsev AV, et al. Mechanisms of wave fractionation at boundaries of high-frequency excitation in the posterior left atrium of the isolated sheep heart during atrial fibrillation. Circulation. 2006; 113:626–633. [PubMed: 16461834]
13. Mandapati R, Skanes A, Chen J, Berenfeld O, Jalife J. Stable microreentrant sources as a mechanism of atrial fibrillation in the isolated sheep heart. Circulation. 2000; 101:194–199. [PubMed: 10637208]
14. Mansour M, Mandapati R, Berenfeld O, Chen J, Samie FH, Jalife J. Left-to-right gradient of atrial frequencies during acute atrial fibrillation in the isolated sheep heart. Circulation. 2001; 103:2631–2636. [PubMed: 11382735]
15. Skanes AC, Mandapati R, Berenfeld O, Davidenko JM, Jalife J. Spatiotemporal periodicity during atrial fibrillation in the isolated sheep heart. Circulation. 1998; 98:1236–1248. [PubMed: 9743516]
16. Atienza F, Martins RP, Jalife J. Translational research in atrial fibrillation: A quest for mechanistically based diagnosis and therapy. Circulation. Arrhythmia and electrophysiology. 2012; 5:1207–1215. [PubMed: 23022707]
17. Atienza F, Almendral J, Jalife J, et al. Real-time dominant frequency mapping and ablation of dominant frequency sites in atrial fibrillation with left-to-right frequency gradients predicts long-term maintenance of sinus rhythm. Heart rhythm : the official journal of the Heart Rhythm Society. 2009; 6:33–40. [PubMed: 19121797]

18. Atienza F, Almendral J, Moreno J, et al. Activation of inward rectifier potassium channels accelerates atrial fibrillation in humans: Evidence for a reentrant mechanism. Circulation. 2006; 114:2434–2442. [PubMed: 17101853]
19. Sanders P, Berenfeld O, Hocini M, et al. Spectral analysis identifies sites of high-frequency activity maintaining atrial fibrillation in humans. Circulation. 2005; 112:789–797. [PubMed: 16061740]
20. Atienza F, Calvo D, Almendral J, et al. Mechanisms of fractionated electrograms formation in the posterior left atrium during paroxysmal atrial fibrillation in humans. Journal of the American College of Cardiology. 2011; 57:1081–1092. [PubMed: 21349400]
21. Jais P, Haissaguerre M, Shah DC, Chouairi S, Gencel L, Hocini M, Clementy J. A focal source of atrial fibrillation treated by discrete radiofrequency ablation. Circulation. 1997; 95:572–576. [PubMed: 9024141]
22. Narayan SM, Krummen DE, Clopton P, Shivkumar K, Miller JM. Direct or coincidental elimination of stable rotors or focal sources may explain successful atrial fibrillation ablation: On-treatment analysis of the confirm trial (conventional ablation for af with or without focal impulse and rotor modulation). Journal of the American College of Cardiology. 2013; 62:138–147. [PubMed: 23563126]
23. Narayan SM, Krummen DE, Shivkumar K, Clopton P, Rappel WJ, Miller JM. Treatment of atrial fibrillation by the ablation of localized sources: Confirm (conventional ablation for atrial fibrillation with or without focal impulse and rotor modulation) trial. Journal of the American College of Cardiology. 2012; 60:628–636. [PubMed: 22818076]
24. Miller JM, Kowal RC, Swarup V, et al. Initial independent outcomes from focal impulse and rotor modulation ablation for atrial fibrillation: Multicenter firm registry. Journal of cardiovascular electrophysiology. 2014; 25:921–929. [PubMed: 24948520]
25. Dixit S, Gerstenfeld EP, Ratcliffe SJ, et al. Single procedure efficacy of isolating all versus arrhythmogenic pulmonary veins on long-term control of atrial fibrillation: A prospective randomized study. Heart rhythm : the official journal of the Heart Rhythm Society. 2008; 5:174–181. [PubMed: 18242535]
26. Atienza F, Almendral J, Ormaetxe JM, et al. Radar-af investigators. Multicenter comparison of radiofrequency catheter ablation of drivers versus circumferential pulmonary vein isolation in patients with atrial fibrillation. A noninferiority randomized clinical trial. Journal of the American College of Cardiology. 2014 In press.
27. Gerstenfeld EP, SippensGroenewegen A, Lux RL, Lesh MD. Derivation of an optimal lead set for measuring ectopic atrial activation from the pulmonary veins by using body surface mapping. Journal of electrocardiology. 2000; 33(Suppl):179–185. [PubMed: 11265719]
28. Berenfeld O. Toward discerning the mechanisms of atrial fibrillation from surface electrocardiogram and spectral analysis. Journal of electrocardiology. 2010; 43:509–514. [PubMed: 20673913]
29. Guillem MS, Climent AM, Millet J, et al. Noninvasive localization of maximal frequency sites of atrial fibrillation by body surface potential mapping. Circulation. Arrhythmia and electrophysiology. 2013; 6:294–301. [PubMed: 23443619]
30. Rodrigo M, Guillem MS, Climent AM, et al. Body surface localization of left and right atrial high-frequency rotors in atrial fibrillation patients: A clinical-computational study. Heart Rhythm. 2014; 11(9):1584–91. [PubMed: 24846374]
31. Guillem MS, Climent AM, Castells F, Husser D, Millet J, Arya A, Piorkowski C, Bollmann A. Noninvasive mapping of human atrial fibrillation. J Cardiovasc.Electrophysiol. 2009; 20:507–513. [PubMed: 19017334]
32. Berenfeld O. Quantifying activation frequency in atrial fibrillation to establish underlying mechanisms and ablation guidance. Heart Rhythm. 2007; 4:1225–1234. [PubMed: 17765627]

Key Points

- Atrial fibrillation (AF) maintenance in experiments and certain groups of patients depends on localized reentrant sources with fibrillatory conduction to the remainder of the atria.
- AF can be eliminated by directly ablating AF-driving sources or “rotors” that exhibit high-frequency, periodic activity.
- The RADAR-AF randomized clinical trial demonstrated that in paroxysmal AF patients, selective ablation of highest frequency sites responsible for AF maintenance is as effective as CPVI, and decreased ablation risks.
- Body surface potential map dominant frequency estimation allows the global identification of high-frequency sources driving AF before and during the electrophysiology laboratory procedure for ablation.
- Phase maps of HDF-filtered BSPM recordings allow prior and real-time noninvasive localization of atrial re-entries during AF, enabling further physiologically-based rationale for personalized AF ablation procedures.

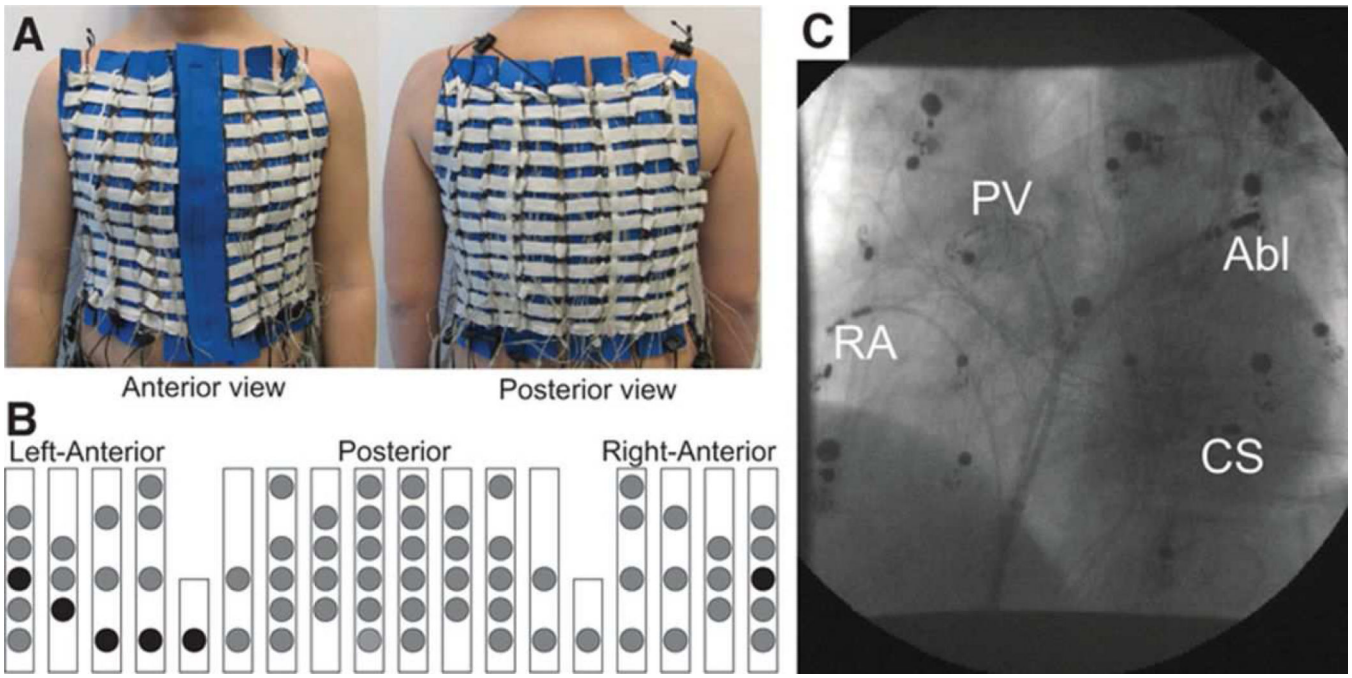

Figure 1.

The setup of the body surface recording electrodes. (A) Anterior and posterior views of the custom-made vest with 64 recording electrodes along vertical blue strips. (B) Schematic location of surface electrodes. Circles represent the location of recording electrodes. Electrodes representing the standard ECG precordial leads are denoted as black circles. (C) X-ray image displaying the locations of the intracardiac recording catheters together with the surface leads. Abl: ablation catheter; PV: Circular mapping at the right superior pulmonary vein; RA: right atrium; CS: coronary sinus. (From Guillem MS, Climent AM, Millet J, et al. Noninvasive localization of maximal frequency sites of atrial fibrillation by body surface potential mapping. *Circulation. Arrhythmia and electrophysiology*. 2013;6:294-30; with permission.)

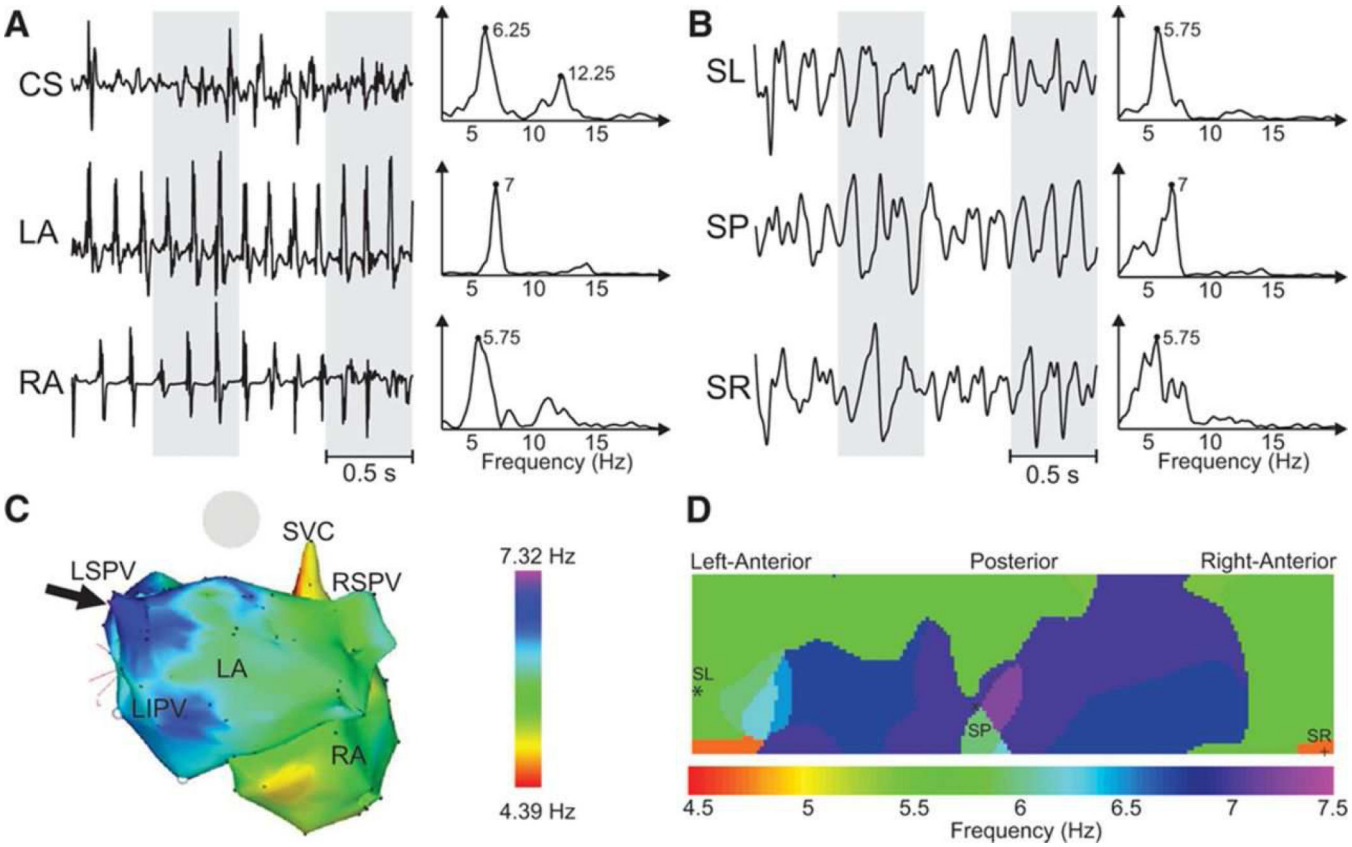

Figure 2.

Recorded EGMs and ECGs and their DF distribution in a sample patient with a left-to-right DF gradient. (A) Three examples of EGMs recorded at different atrial sites and their corresponding power spectra. (B) Selected surface BSPM leads: Surface Left (SL), Surface Posterior (SP) and Surface Right (SR), and their corresponding power spectra. (C) Intracardiac DF map. Black arrow points to the LA region with highest DF at the LSPV. (D) DF map on the torso surface with superimposed locations of electrodes from (B). (From Guillem MS, Climent AM, Millet J, et al. Noninvasive localization of maximal frequency sites of atrial fibrillation by body surface potential mapping. *Circulation. Arrhythmia and electrophysiology*. 2013;6:294-30; with permission.)

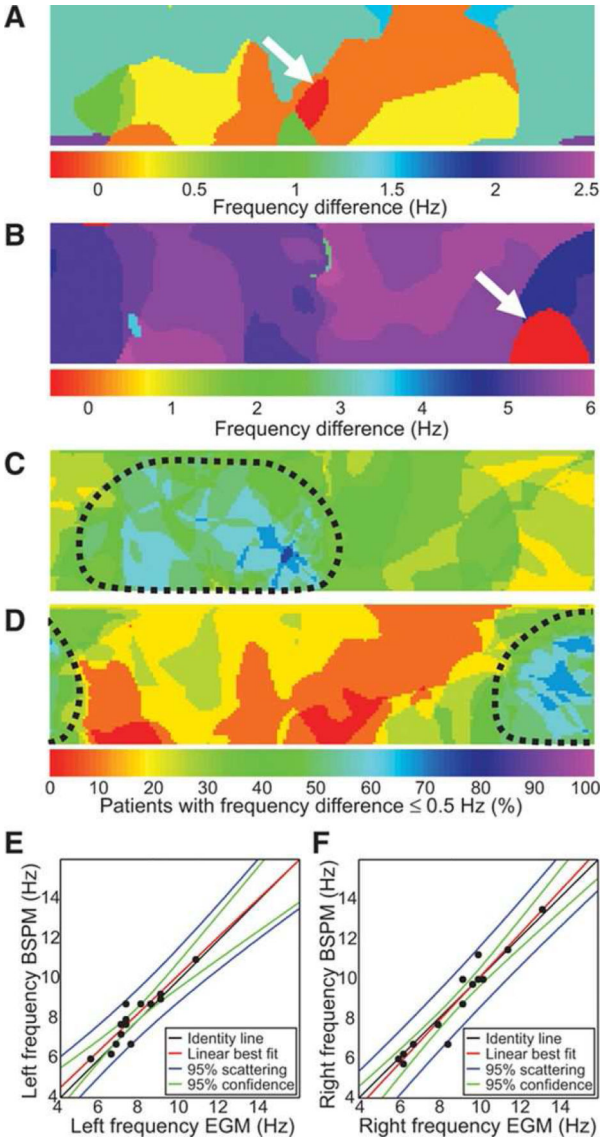

Figure 3.

Correspondence between intracardiac and surface dominant frequency (DFs). (A,B) Differences between maximum intracardiac eletrogram (EGM) DF and local surface DF represented in a color scale for two different patients. The red color domain on the surface (white arrows) represents the region with zero difference between the intracardiac and surface DFs. (A)Patient from Figure 2 with a left-to-right DF gradient.(B) Patient with a right-to-left DF gradient.(C,D) Summary maps showing the percent patients with the surface DFs less than 0.5 Hz different than the maximal left (C) and maximal right (D) intracardiac DFs. Areas outlined by the dashed curves represent the portion of the torso with a best correspondence with left and right EGMs. (E) Correlation plot showing highest DFs found in left EGMs vs. highest DFs found on the left portion of the torso. (F) Correlation plot showing highest DFs found in right EGMs vs. highest DFs found on the right portion of the torso. (From Guillem MS, Climent AM, Millet J, et al. Noninvasive localization of maximal

frequency sites of atrial fibrillation by body surface potential mapping. *Circulation. Arrhythmia and electrophysiology*. 2013;6:294-30; with permission.)

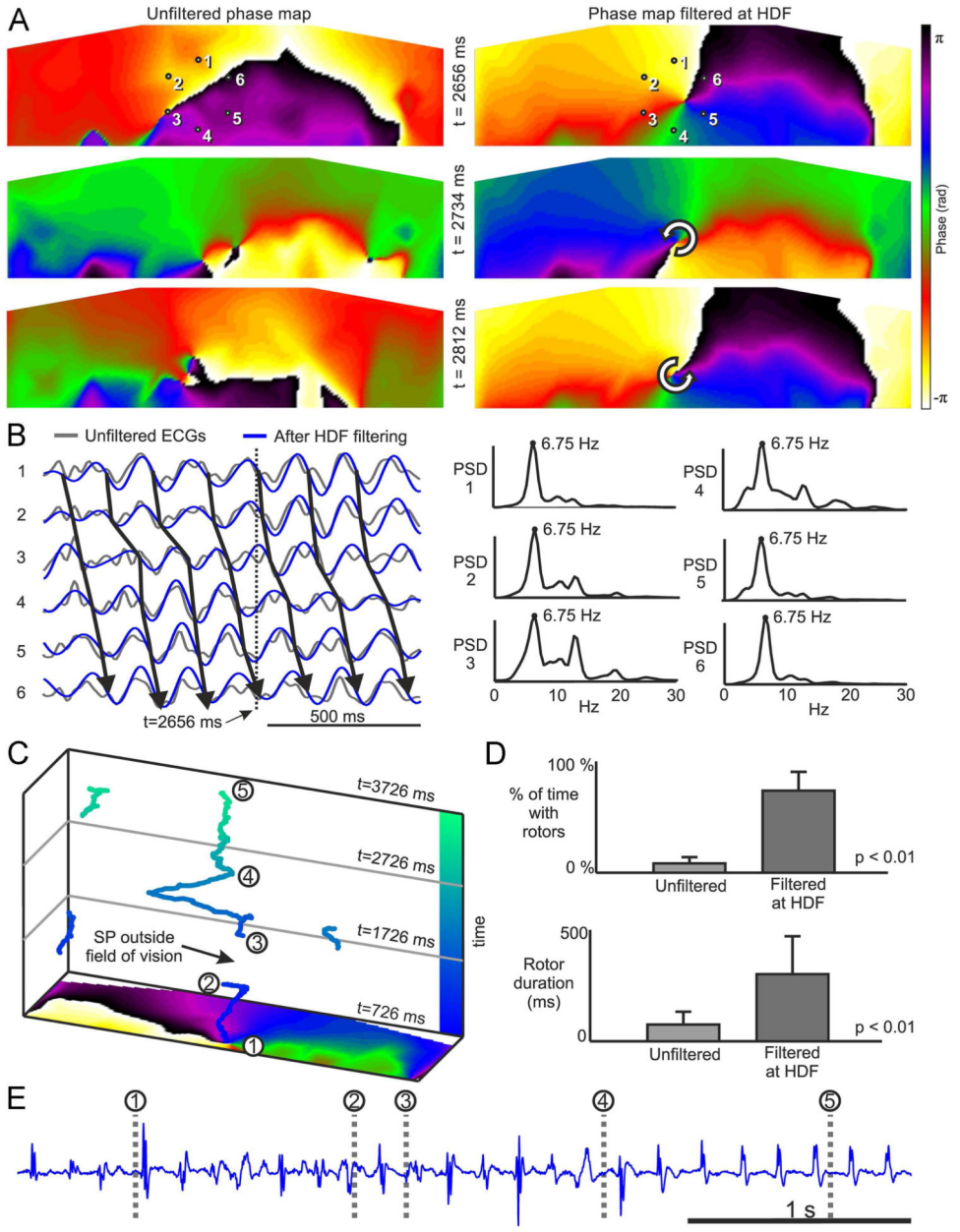

Figure 4.

Surface phase maps during AF. (A) Surface phase maps at three selected times for unfiltered (left) and for HDF-filtered (right) surface potentials. (B) ECGs at positions 1-6 marked in panel A before and after HDF-filtering and Power Spectral Density (PSD) for unfiltered ECGs. Time marker at 2656 ms corresponds to the top map in the HDF-filtered data in panel A. (C) PSs trajectories on the torso surface during a 3-sec long AF. (D) Percentage of time with rotors (up) and rotor duration (down) in surface phase maps from unfiltered and HDF-filtered surface potentials over the entire cohort. (E) Electrogram recorded at the highest DF site in the atria (RSPV) simultaneously with the surface recordings. (From Rodrigo M, Guillem MS, Climent AM, et al. Body surface localization of left and right atrial high-

frequency rotors in atrial fibrillation patients: A clinical-computational study. *Heart Rhythm* 2014; 11(9):1584–91;with permission.)

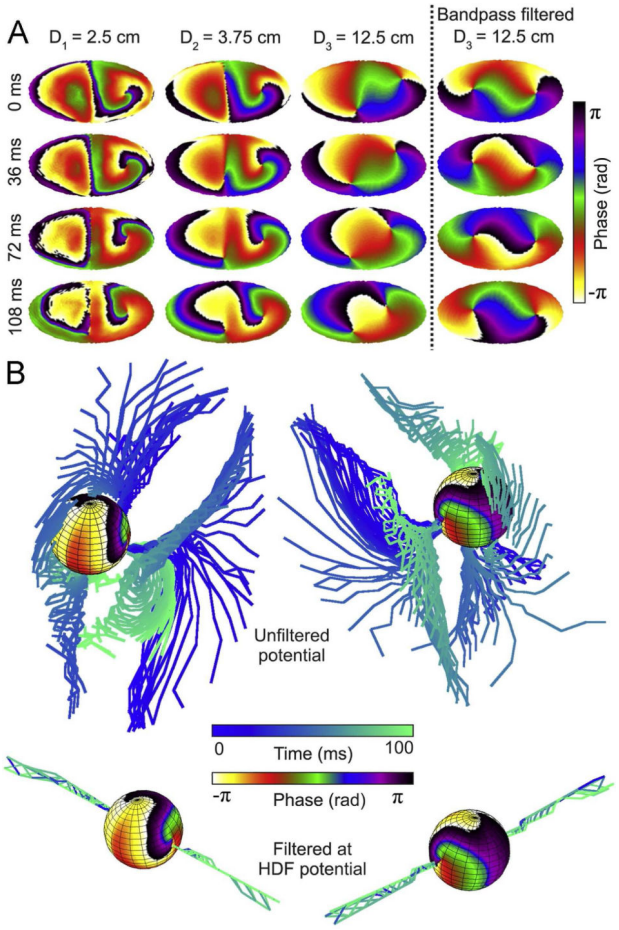

Figure 5.

Epicardial and transition to surface phase maps during AF in a 50% LA–50% RA atrial model. (A) Phase maps at 4 time instants (top to down) in 3 concentric layers at increasing distances from the epicardium (left to right) and after HDF filtering of surface potentials. (B) Phase map of epicardial sphere and temporal distribution of filaments for unfiltered potentials and for HDF-filtered potentials. (Adapted from Rodrigo M, Guillem MS, Climent AM, et al. Body surface localization of left and right atrial high-frequency rotors in atrial fibrillation patients: A clinical-computational study. *Heart Rhythm* 2014; 11(9):1584–91;with permission.)

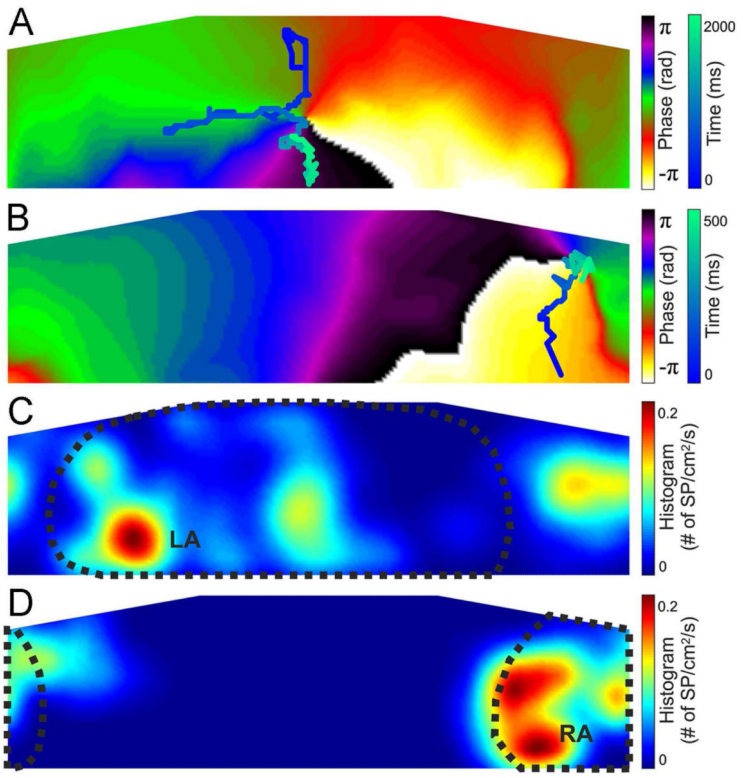

Figure 6.

Spatial distribution of surface rotors in human AF. (A) Phase map and rotor tracking (blue scale) after LA-HDF filtering in an LA-fastest patient. (B) Phase map and rotor tracking (blue scale) after RA-HDF filtering in an RA-fastest patient. (C) Histogram of the rotor position for all rotors detected in patients with an inter-atrial DF gradient after LA-HDF filtering. LA-detected region is outlined with a dotted line. (D) Histogram of the rotor position for all rotors detected in patients with an inter-atrial DF gradient after RA-HDF filtering. RA-detected region is outlined with a dotted line. (From Rodrigo M, Guillem MS, Climent AM, et al. Body surface localization of left and right atrial high-frequency rotors in atrial fibrillation patients: A clinical-computational study. *Heart Rhythm* 2014; 11(9):1584–91;with permission.)